Sains Malaysiana 52(1)(2023): 129-138
http://doi.org/10.17576/jsm-2023-5201-10

Adsorption Isotherm and Surface Analysis for the Carbonate Formation on Nano Coral-Shaped Iron(Iii) Oxide

(Isoterma Penjerapan dan Analisis Permukaan bagi Pembentukan Karbonat di atas Ferum(Iii) Oksida Berbentuk Karang Nano)

AZIZUL HAKIM LAHURI[1,*], MOHD AMBAR YARMO[2], NORAZZIZI NORDIN[3], NORLIZA DZAKARIA[4], ADELINE HWONG ING ING[5] & SOPHIA JELINA STANLEY KUDA[5]

[1]Department of Science and Technology, Universiti Putra Malaysia Bintulu Kampus, Nyabau Road, P.O Box 396, 97008 Bintulu, Sarawak, Malaysia
[2]Department of Chemical Sciences, Faculty of Science and Technology, Universiti Kebangsaan Malaysia, 43600 UKM Bangi, Selangor Darul Ehsan, Malaysia
[3]School of Chemical Sciences, Universiti Sains Malaysia, 11800 Gelugor, Pulau Pinang, Malaysia
[4]School of Chemistry and Environment, Faculty of Applied Sciences, Universiti Teknologi MARA, Cawangan Negeri Sembilan, Kampus Kuala Pilah, Pekan Parit Tinggi, 72000 Kuala Pilah, Negeri Sembilan Darul Khusus, Malaysia
[5]Faculty of Resource Science and Technology, Universiti Malaysia Sarawak, 94300 Kota Samarahan, Sarawak, Malaysia

Received: 22 March 2022/Accepted: 25 June 2022

ABSTRACT

The α-Fe_2O_3 was synthesized using the hydrolysis method to obtain the nano coral-shaped morphology. The adsorption isotherm and surface analysis upon CO_2 adsorption were identified. The adsorption capacity for nano coral-shaped α-Fe_2O_3 was measured at 8.66 cm^3/g (17.00 mg/g). Experimental data from CO_2 adsorption isotherm at 25 °C best fits with the Freundlich isotherm model which implies the adsorption process is favorable and the multilayer adsorption on the heterogeneous surface. A decrease in the α-Fe_2O_3 crystallite peaks in the X-ray diffractogram after the CO_2 adsorption was associated with the carbonate complexes species formation. IR spectra indicate higher intensities over the CO_2 exposure time of 4, 12 and 24 h, especially at absorption bands 1041 and 1627 cm^{-1} that corresponded to C-O and asymmetry O-C-O stretches, respectively, for carbonate. The morphology of the carbonate formation on nano coral-shaped α-Fe_2O_3 over the CO_2 exposure time was analyzed using FESEM-EDX. Although the carbonate formation was not distinct, the increment in the C element also confirmed the capability of the α-Fe_2O_3 in adsorbing CO_2 for a long adsorption time of 24 h.

Keywords: Adsorption isotherm; carbonate formation; CO_2 capture; hydrolysis method; iron(III) oxide

ABSTRAK

α-Fe_2O_3 telah disintesis menggunakan kaedah hidrolisis untuk mendapatkan morfologi berbentuk nano karang. Isoterma penjerapan dan analisis permukaan terhadap penjerapan CO_2 telah dikenal pasti. Keupayaan penjerapan bagi α-Fe_2O_3 berbentuk nano karang telah diperoleh sebanyak 8.66 cm^3/g (17.00 mg/g). Isoterma penjerapan CO_2 pada 25 °C daripada data uji kaji paling sesuai dengan model isoterma Freundlich menunjukkan proses penjerapan adalah berlaku dengan mudah dan penjerapan lapisan berganda pada permukaan yang heterogen. Penurunan puncak kekisi α-Fe_2O_3 dalam difraktogram sinar X selepas penjerapan CO_2 adalah dikaitkan dengan pembentukan spesies karbonat kompleks. Spektrum IR menunjukkan keamatan yang lebih tinggi terhadap masa pendedahan CO_2 pada 4, 12 dan 24 jam, terutamanya pada jalur-jalur serapan bagi 1041 dan 1627 cm^{-1} yang masing-masing sepadan dengan regangan C-O dan O-C-O tak simetri bagi karbonat. Morfologi bagi pembentukan karbonat di atas α-Fe_2O_3 berbentuk nano karang terhadap masa pendedahan CO_2 dianalisis menggunakan FESEM-EDX. Walaupun pembentukan karbonat adalah tidak jelas, peningkatan unsur C juga telah mengesahkan keupayaan α-Fe_2O_3 dalam menjerap CO_2 dalam masa penjerapan yang panjang pada 24 jam.

Kata kunci: Ferum(III) oksida; isoterma penjerapan; kaedah hidrolisis; pembentukan karbonat; penjerapan CO_2

Introduction

Numerous iron oxide synthesis methods were reported to obtain nanoparticles and controlled shape. Besides physical and biological methods, chemical methods such as thermal decomposition, hydrothermal, co-precipitation, sol-gel, hydrolysis, electrochemical and microemulsion were commonly reported for iron oxide synthesis (Andrade, Veloso & Castanheira 2020). Whereas metal oxides (Fe_2O_3, Bi_2O_3, CeO_2, Co_3O_4, ZnO, NiO) deposited on other metal oxide or support materials applying the impregnation method (Hakim et al. 2015a, 2015b; Lahuri et al. 2022a, 2020a, 2020b). Generally, the hydrolysis method is the initial pathway for hydrothermal, sol-gel and co-precipitate methods (Zhong et al. 2012). This method would be the simplest, economically safe and less using hazardous chemicals.

In the hydrolysis method, the metal ions form aqua coordination complexes $[Fe(H_2O)_6]^{3+}$ in which the hydrolysis reaction takes place in water or aqueous solutions as shown in Equation (1). A selected non-aqueous solvent such as ethanol is applied as a stabilizer (Hakim et al. 2016c). This method does not form a gel structure due to no addition of shaping agents such as a polymer (polyethylene glycol, polyethyleneimene) and surfactant (oleyamine, octadecylamine) (Andrade, Veloso & Castanheira 2020). Usually, the shaping agent forms a hydrogen bond as a linkage that influences the shape, morphology and particle growth. However, a simpler ethanol molecule also could form a linkage of hydrogen bond between hydrate of the salt. The final process of calcination is the thermal treatment is significant to the geometrical and crystal structure of the particle.

$$[Fe(H_2O)_6]^{3+} + H_2O \rightarrow [Fe(OH)(H_2O)_5]^{2+} + H_3O^+ \quad (1)$$

The particle shape can be controlled kinetically or thermodynamically. In the thermodynamic process, the chemical reaction potential is associated with controllable parameters such as supersaturation of the solution and temperature. Whereas the kinetic process involves stable nucleation sites in supersaturated regions in which reduce the reaction energy barrier (Wu, Yang & Wu 2016). During the particle growth by thermodynamically driven, the reaction favors reducing the particle's surface free energy (Lisjak & Mertejeli 2018). It involves two significant mechanisms that influence the rate of deposition of atoms in the nuclei's surface. The two mechanisms are reaction-limited and diffusion-limited which correspond to low and high solution concentrations, respectively. At low solution concentration, the reaction-limited take place as the particle growth toward its final shapes are depending on the surface reaction limit. At high concentrations, the diffusion-limited is due to the monomers being precipitated on the particle surfaces which favor the monodisperse nanoparticles. Thus, the final shape is affected by synthesis parameters such as solvent, temperature, precursor concentration and pH (Shaba et al. 2021).

The particle shape also exhibits different activity toward CO_2 adsorption capacity. The mesoporous silica in rod-shaped exhibited higher surface area and CO_2 adsorption capacity compared to spherical-shaped (Khdary et al. 2018). The ethylene glycol was added as a shaping agent to obtain rod-shaped mesoporous silica, while spherical-shaped was synthesized without ethylene glycol. A nanowire morphology of lithium silicate was synthesized using plasma oxidation exhibiting ultrafast CO_2 adsorption in 3 minutes with an adsorption capacity of 25 wt. % (Nambo 2019). A chemical precipitation method was applied to obtain the spherical shape of α-Fe_2O_3 nanoparticles at 21 nm by using 0.05 M $FeCl_3.6H_2O$ as a precursor (Lassoued et al. 2017). Meanwhile, an ultrasonic-assisted hydrolysis technique using ammonium bicarbonate as the precipitation agent and phosphoric acid as pH controller also resulted in uniform spherical shape α-Fe_2O_3 with an average particle size of 50 nm (Chen, Chen & Liu 2016). Nonetheless, the synthesis method for α-Fe_2O_3 toward CO_2 capture activity is not widely explored.

Therefore, this work attempt to study the CO_2 adsorption activity through the carbonate formation onto α-Fe_2O_3 which is synthesized by the hydrolysis method. This extended work from Hakim et al. (2016b) emphasizes the long period of CO_2 exposure onto the particle shape generated by the hydrolysis method. The adsorption mechanism will be analyzed by applying the experimental CO_2 adsorption isotherm at 25 °C to the adsorption isotherm models. The carbonate formation on α-Fe_2O_3 will be observed using Fourier transform infrared (FTIR) spectroscopy and field emission scanning electron microscope equipped with energy dispersive X-ray (FESEM-EDX).

Materials and Methods

The synthesis method was adapted from Hakim et al. (2016b). The ethanol (C_2H_5OH, 99.7%) was obtained from Systerm, Malaysia, while iron(III) nitrate nonahydrate ($Fe(NO_3)_3 \cdot 9H_2O$, 98%) from Sigma-Aldrich,

USA. The bulk α-Fe_2O_3 was purchased from BDH, United Kingdom. Pre-treatment was performed by calcining the bulk α-Fe_2O in a nitrogen atmosphere at 150 °C for 1 hour. Briefly, the precursor of $Fe(NO_3)_3 \cdot 9H_2O$ was dissolved in distilled water to have a concentration of 2 M solution. The ethanol was added to the solution with a volume percentage of 25% from the distilled water used. The mixture was stirred for 1 hour at room temperature and followed by sonicating for 20 minutes. The mixture was dried by stirring at the temperature of 80 - 100 °C. The α-Fe_2O_3 was ground using a mortar and continued to dry in an oven for 24 hours at 110 °C. The α-Fe_2O_3 was calcined under ambient air at the temperature of 450 °C. The precursor concentration and calcination temperature were chosen from the most efficient in CO_2 adsorption capacity from Hakim et al. (2016c).

CO_2 adsorption isotherm at 25 °C was measured using a static volumetric technique from a gas sorption analyzer, Micromeritics ASAP 2020. Approximately 500 mg sample was outgassed for 6 hours at 200 °C. The CO_2 adsorption was conducted in a circulating water bath to control the adsorption temperature of 25 °C. The CO_2 adsorption isotherm data will be analyzed using the linearized form of Langmuir, Freundlich, Temkin and Dubinin-Radushkevich (D-R) isotherm models.

The composition of the α-Fe_2O_3 and bulk α-Fe_2O_3 was characterized using surface analysis of X-ray Diffraction (XRD) with Bruker AXS D8 Advance type. The diffraction angle was recorded from 20° to 90°. The composition was identified by matching with standard diffraction data (JCPDS). The carbonate formation on α-Fe_2O_3 was analyzed by XRD to compare the crystalline phase composition. Meanwhile, the carbonate formation was conducted using temperature programmed desorption CO_2 (CO_2-TPD) from a chemisorption analyzer model Micromeritics 2920 Chemisorb. Approximately 50 mg of α-Fe_2O_3 has treated heat exposure in an inert atmosphere of He flow at 150 °C for 30 minutes to eliminate traces of moisture and humidity gases. When the furnace temperature was cooled to 30 °C, the gas feed was switched to a mixture of 5 % (V/V) CO_2 in He to perform the CO_2 adsorption by saturating flow for 1 hour. The mixture gas was switched to He for 30 minutes with a flow rate of at 50 °C to remove the weak adsorbed CO_2. It was followed by the desorption process at elevated temperatures from 30 to 650 °C. The method was performed separately until the adsorption process and desorption process. After the reaction, the α-Fe_2O_3 sample was collected to analyze using XRD.

The surface chemistry of the carbonate formation on the α-Fe_2O_3 was studied by using FTIR spectroscopy and FESEM-EDX. The reaction was conducted using a fluidized bed reactor. Approximately 4 g of the α-Fe_2O_3 was placed in the column. The fresh sample was cleaned by flowing N_2 at 150 °C for 30 minutes prior to CO_2 exposure for 4, 12 and 24 hours separately, at 30 °C. The bulk α-Fe_2O_3, fresh α-Fe_2O_3 and after being exposed to CO_2 were analyzed using FTIR spectroscopy and FESEM-EDX. The trend of the carbonate formation on α-Fe_2O_3 could be observed over time through the presence of functional groups using FTIR spectroscopy from a Perkin Elmer model GX. The sample is prepared by KBr pellet techniques mixing the sample with KBr. The wavenumbers of the spectra obtained from the FTIR method are between the range of 450 cm^{-1} to 4000 cm^{-1}. Whereas, the morphology and elemental analyses of the fresh α-Fe_2O_3 and carbonate formation were evaluated using FESEM-EDX (ZEISS Supram™ 55).

RESULTS AND DISCUSSION

The CO_2 adsorption isotherm at 25 °C is shown in Figure 1. A significant difference in the adsorption capacity between α-Fe_2O_3 and bulk α-Fe_2O_3, which α-Fe_2O_3 exhibits the adsorption capacity of 8.66 cm^3/g (17.00 mg/g) compared to bulk α-Fe_2O_3 at 1.53 cm^3/g (3.00 mg/g). Although this value is slightly lower than amine-functionalized solid sorbent (Abu Tahari et al. 2020, 2017), amine-based materials face several drawbacks such as causing equipment corrosion and removal of amine compound during the desorption process that reduces the sorption capacity. The hydrolysis method generates a higher surface area and trimodal pore size distribution for α-Fe_2O_3 compared to the bulk α-Fe_2O_3 (Hakim et al. 2016c). This would be the reason for an abrupt increase in the adsorption capacity, which more space to occupy the CO_2. Hence, a further analysis was studied to provide an insightful understanding of the adsorption mechanism.

The adsorption mechanism was evaluated by analyzing the experimental data for CO_2 adsorption isotherm at 25 °C with adsorption isotherm models such as Langmuir, Freundlich, Temkin and D-R. The linearized form of the adsorption isotherm models are shown in Figure 2 and their parameters are tabulated in Table 1. The Langmuir isotherm model best describes gas-solid phase adsorption, the dynamic equilibrium of the surface adsorption and comparing the approximate adsorption capacity (Lahuri et al. 2022c). The experimental data

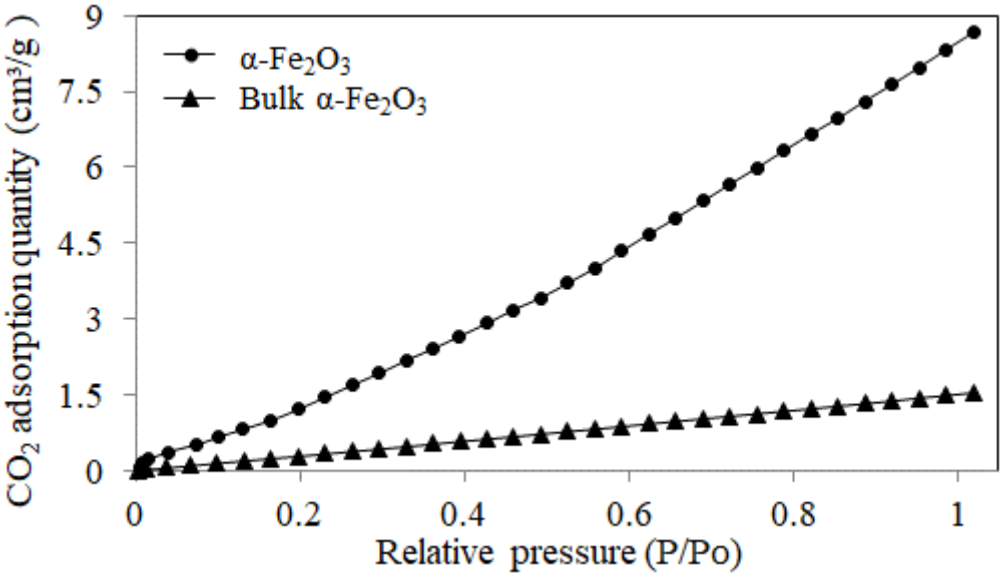

FIGURE 1. CO_2 adsorption isotherm at 25 °C

fit well with the Langmuir isotherm with R^2 = 0.4243. The theoretical adsorption quantity ($Q_\circ$ = 3.497 cm^3/g) and adsorption energy (K_L = 0.8252) were calculated from the slope and intercept respectively. It explains the maximum adsorption that refers to a saturated monolayer of CO_2 molecules on the adsorbent surfaces without transmission of adsorbate in the plane of the adsorbate surface. Based on the results, $Q_\circ$ deviates from the experimental value but the CO_2 adsorption is favorable due to the dimensionless separation factor (R_L = 2.885 × 10^{-6}) within the range of 0-1 (Lahuri et al. 2020c).

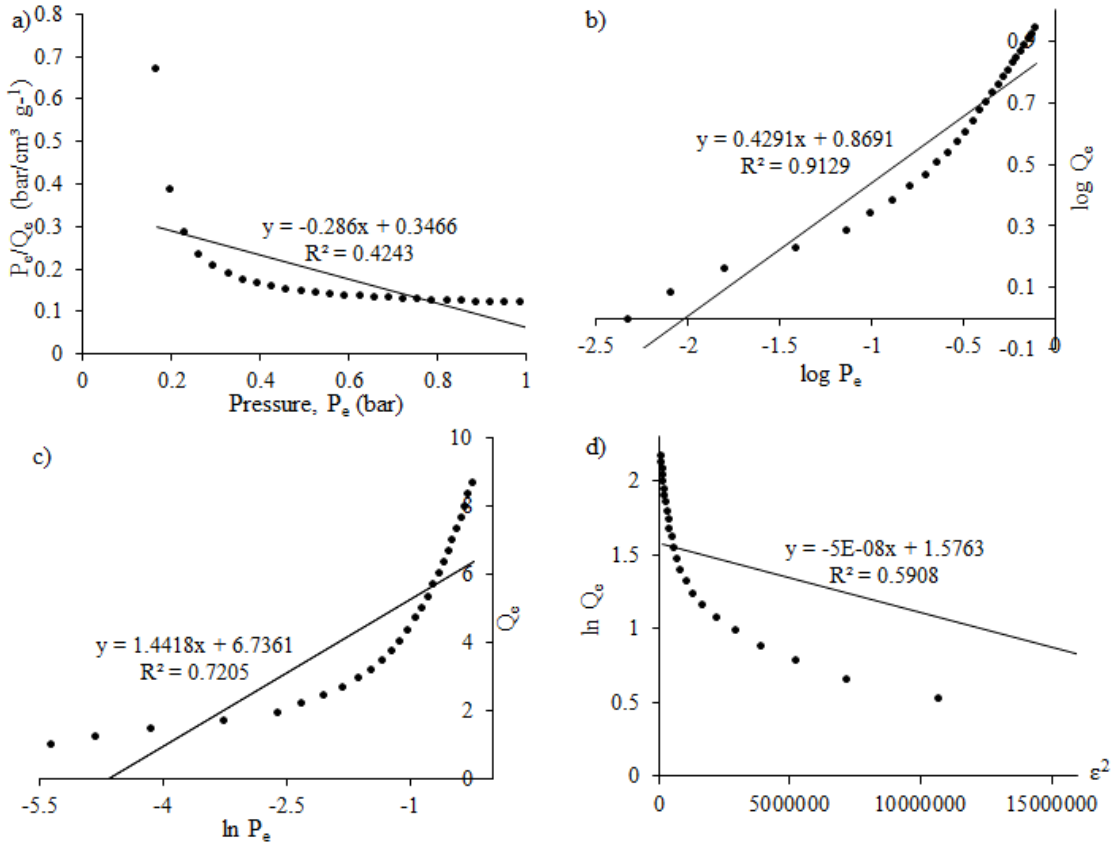

FIGURE 2. Adsorption isotherms by a) Langmuir, b) Freundlich, c) Temkin and d) D-R models in linearized form using CO_2 adsorption isotherm at 25 °C for α-Fe_2O_3

The Freundlich isotherm exhibits the best fit with the experimental data with $R^2 = 0.9129$ and the theoretical adsorption quantity (K_F = 7.398 $cm^3/g \cdot bar^{1/n}$) closest to the experimental adsorption quantity. When the number of molecules bound to the adsorption site increases, smaller chances of molecule binding at the same sites due to higher energy is required to allow another molecule to bind at the same adsorption sites (Lahuri et al. 2022c; Rashidi & Yusup 2017). Therefore, this model assumes multilayer adsorption onto a heterogeneous surface that is ascribed to the physicochemical properties of active sites and adsorbed molecules (Ammendola, Raganati & Chirone 2017). The adsorption does not comply with driving force or cooperative adsorption attributed to the $1/n$ value of 0.429, which is $1/n < 1$ suggests greater heterogeneity when the smaller the value (Ammendola, Raganati & Chiro 2017; Lahuri et al. 2022c). This model also suggests a favorable adsorption process with the Freundlich constant of $n = 2.330$ which is $n > 1$.

For the Temkin isotherm model, it derives the surface coverage linearly proportional with the heat of adsorption for all molecules in the layer (Lahuri et al. 2022c). The parameters of the model are bond constant (A_T = 106.91 L/g) corresponds to the maximum binding energy and heat of adsorption (b_T = 1718.39 J/mol). Meanwhile, the D-R isotherm constant (K_{ad} = 5.0 x 10^{-8} mol^2/J^2) is associated with the mean energy of sorption as it is transferred from the adsorbate to the surface of the adsorbent. This model could obtain the mean free energy (E = 3162.28.14) which both b_T and E from Temkin and D-R model, respectively, are below 8 kJ/mol, suggesting the adsorption is physical in nature (Djomgoue et al. 2012). Although the correlation coefficient of R^2 for Temkin and D-R isotherm are fitted well, the theoretical isotherm saturation capacity (Q_s = 4.837 cm^3/g) deviates from the experimental value.

Based on the R^2 values, the Freundlich isotherm model is fit better with the experimental CO_2 adsorption data and best describes the adsorption process. Thus, the CO_2 adsorption process implies multilayer adsorption on the heterogeneous surfaces of α-Fe_2O_3.

TABLE 1. The adsorption isotherm parameters for Langmuir, Freundlich, Temkin and D-R models using CO_2 adsorption isotherm at 25 °C for α-Fe_2O_3

Isotherm	Plot	Parameters	Values
Langmuir			
Non-linear equation		$Q_{\circ\ cal.}$ (cm^3/g)	3.497
		K_L	0.8252
Linear equation		R_L	2.885×10^{-6}
$P_e/Q_e = 1/Q_\circ K_L + P_e/Q_\circ$	P_e/Q_e against P_e	R^2	0.4243
Freundlich			
Non-linear equation		K_F ($cm^3/g \cdot bar^{1/n}$)	7.398
		$1/n$, (n)	0.429, (2.330)
Linear equation		R^2	0.9129
$\log Q_e = 1/n \log P_e + \log K_F$	$\log Q_e$ vs. $\log P_e$		
Temkin			
Non-linear equation		A_T (L/g)	106.91
		b_T (J/mol)	1718.39
Linear equation		B	1.4418
$Q_e = B \ln A_T + B \ln P_e$	Q_e vs. $\ln P_e$	R^2	0.7205
Dubinin-Radushkevich			
Non-linear equation		Q_s (cm^3/g)	4.837
		K_{ad} (mol^2/J^2)	5.0×10^{-8}
Linear equation		E (J/mol)	3162.28
$\ln Q_e = \ln Q_s - K_{ad}\varepsilon^2$	$\ln Q_e$ vs. ε^2	R^2	0.5908

The X-ray diffractograms are shown in Figure 3. The peaks were observed in all samples correspond to the rhombohedral phase of hematite, α-Fe_2O_3 with lattice parameters a=5.0356 and b=c=13.7489 (matched with JCPDS number 33-0664). A higher intensity of the peaks for α-Fe_2O_3 compared to bulk α-Fe_2O_3 due to more crystallite formation through the hydrolysis method. No additional peaks after being exposed to CO_2, but the peak intensities reduce might be due to the carbonate formation after being exposed to CO_2 for only one hour. It is not similar as $FeCO_3$ since it can be detected by XRD (Mendoza et al. 2019). $Fe_2(CO_3)_3$ formation is thermodynamically unstable due to high polarizing power with high charge density, which is a triply charged ion. Hence, a greater distortion of the carbonate (CO_3^{2-}) ion's electron cloud (Lahuri et al. 2022b). According to Fajan's rule, induced covalent character on ionic compound increases with an increase in charge on the cation, which Fe^{3+} will be less ionic compared to Fe^{2+} (Sattler 2011). The carbonate might be generated in the form of carbonate complexes such as bidentate carbonate (Hakim et al. 2016a). Nevertheless, the reduction in peak intensities is noteworthy to further explore since numerous works reported the potential of α-Fe_2O_3 as a CO_2 adsorbent (Lahuri et al. 2017; Mendoza et al. 2019). After TPD at 650 °C, the peak intensities were slight increases compared to after being exposed to CO_2. This indicates that adsorbed CO_2 was partially removed at 650 °C. The limitation of the XRD analysis should be supported by further surface analyses such as FTIR spectroscopy and FESEM-EDX.

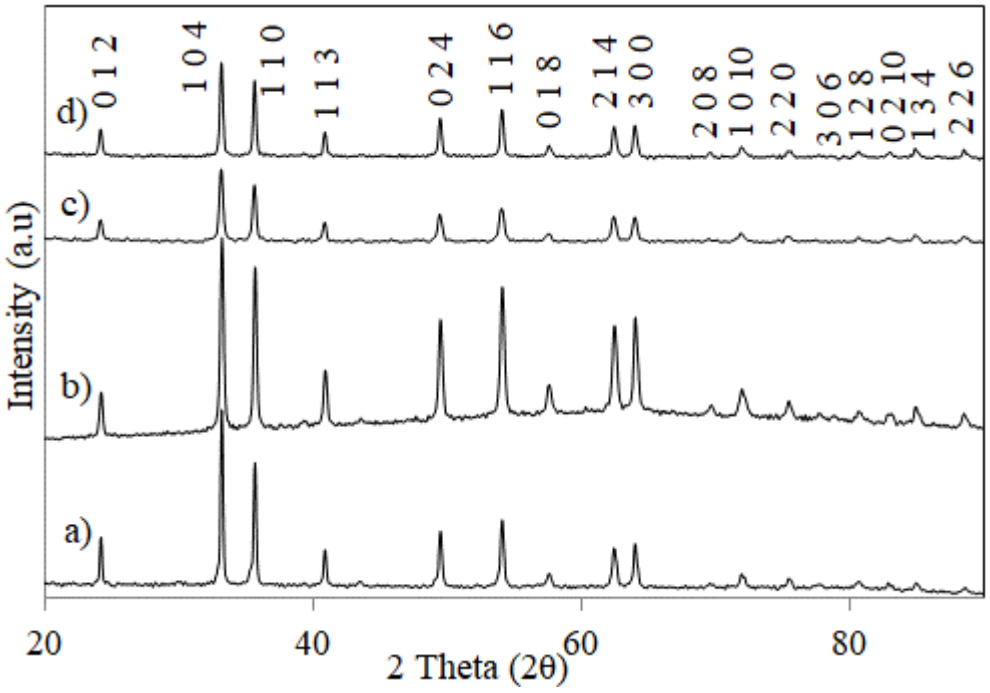

FIGURE 3. XRD pattern for a) bulk α-Fe_2O_3, b) α-Fe_2O_3, c) CO_2 adsorption on α-Fe_2O_3, for 1 hour and d) CO_2-TPD for α-Fe_2O_3 at desorption temperature of 650 °C

The IR spectra for the fresh α-Fe_2O_3 and after CO_2 exposure at 4, 12 and 24 hours are shown in Figure 4. Table 2 shows the vibrational mode assignments of the IR spectra. There is no peak indicating the carbonate formation on bulk α-Fe_2O_3 except the physisorption CO_2 (2347 cm^{-1}) and CO_2 bound to metal ion (2388 cm^{-1}) were appeared for all samples (Lahuri Lahuri & Yarmo 2022b). Unlike bulk α-Fe_2O_3, α-Fe_2O_3 easily adsorb CO_2 from the atmosphere due to the presence of absorption bands of 1041 and 1627 cm^{-1} that are associated with C-O and O-C-O asymmetry stretch, respectively, for carbonate compound (Baltrusaitis et al. 2011: Lahuri & Yarmo 2022b). These peaks were observed to be prominent after 4 hours of CO_2 exposure and onward. A similar trend is

observed for the absorption band at 789 and 915 cm^{-1} that are associated with Fe-O-H (Hakim et al. 2016a, 2016c). A higher intensity of the absorption band of 915 cm^{-1} after 24 h CO_2 adsorption ascribed to the traces moisture content in the gas feed. The absorption bands at 623, 668 and 682 cm^{-1} were assigned for bend CO_2 (Isokoski, Poteet & Linnartz 2013; Kazansky et al. 1999; Mutch et al. 2016). The absorption bands at 423, 443 and 456 cm^{-1} correspond to the Fe-O bond for α-Fe_2O_3 (Mohanraj & Sivakumar 2017; Qin et al. 2011; Tadic et al. 2019). The inconsistency of the fingerprint region in IR spectra might be due to the presence of the moisture content in the sample. The CO_2 exposure could lead to the traces moisture from the gas feed to adsorb onto sample and interfere the Fe-O related peaks. Therefore, the peak intensities that associated with Fe-O-H also increases.

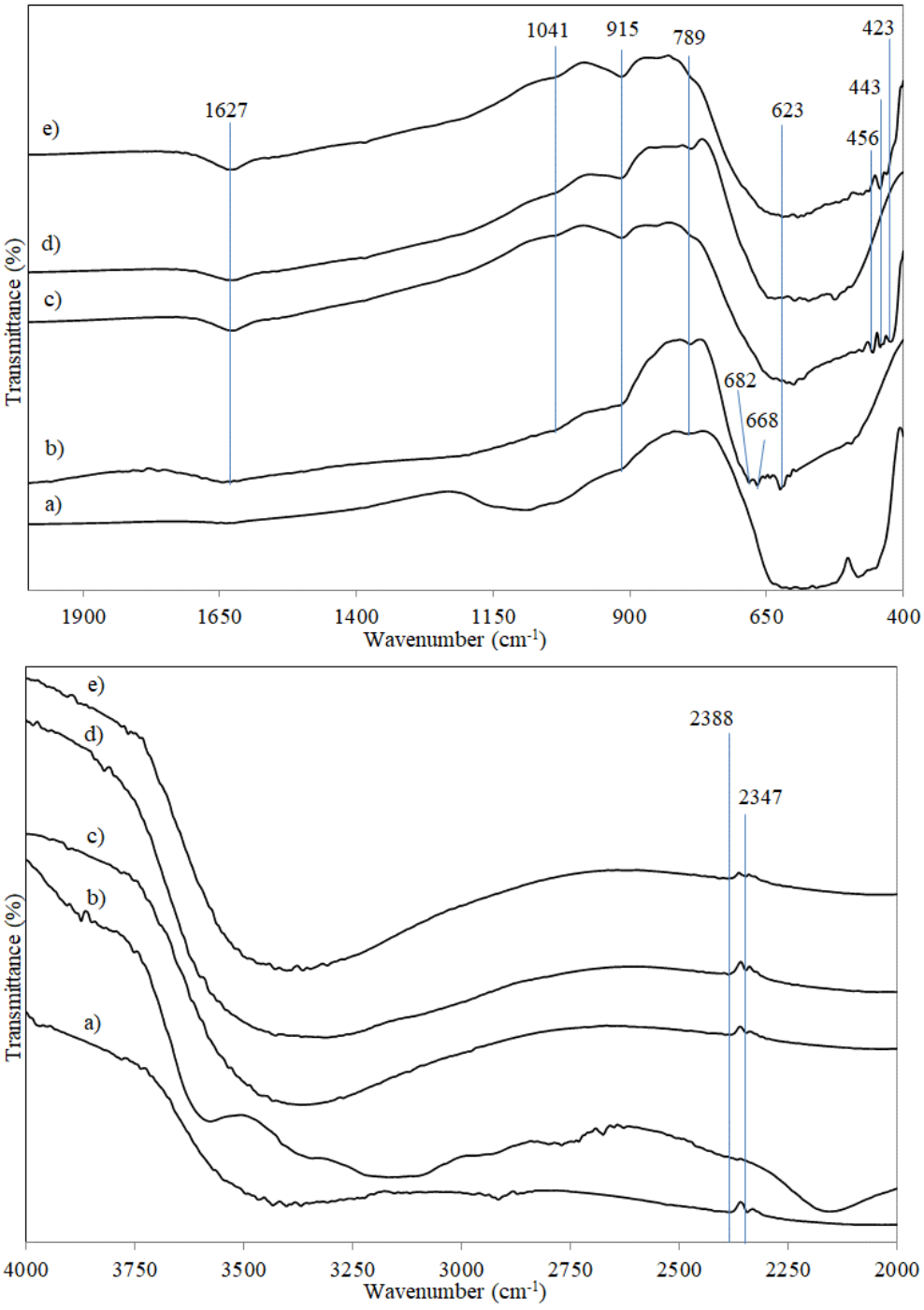

FIGURE 4. IR spectra for a) bulk α-Fe_2O_3, b) α-Fe_2O_3, c) 4 hours of CO_2 adsorption on α-Fe_2O_3, d) 12 hours of CO_2 adsorption on α-Fe_2O_3, e) 24 hours of CO_2 adsorption on α-Fe_2O_3

TABLE 2. Mode assignments of IR absorption bands

Vibrational mode assignments	Experimental frequencies (cm^{-1})	Literature references (cm^{-1})
Fe-O bond	423, 443 and 456	420, 440 and 456
Bend CO_2 (C=O)	623, 668 and 682	625, 666 and 682
Fe-O-H	789, 915	796, 918
C-O	1041	1040
Asymmetry O-C-O	1627	1635
Physisorption CO_2	2347	2344
CO_2 bound to metal ion	2388	2383

Figure 5 shows the morphology of the fresh α-Fe_2O_3 and after being exposed to CO_2 for 4, 12, and 24 hours. The identification of the elemental composition was analyzed quantitatively using EDX. It is noteworthy to observe the α-Fe_2O_3 synthesize by the hydrolysis method generates a nano coral shape. Although a similar

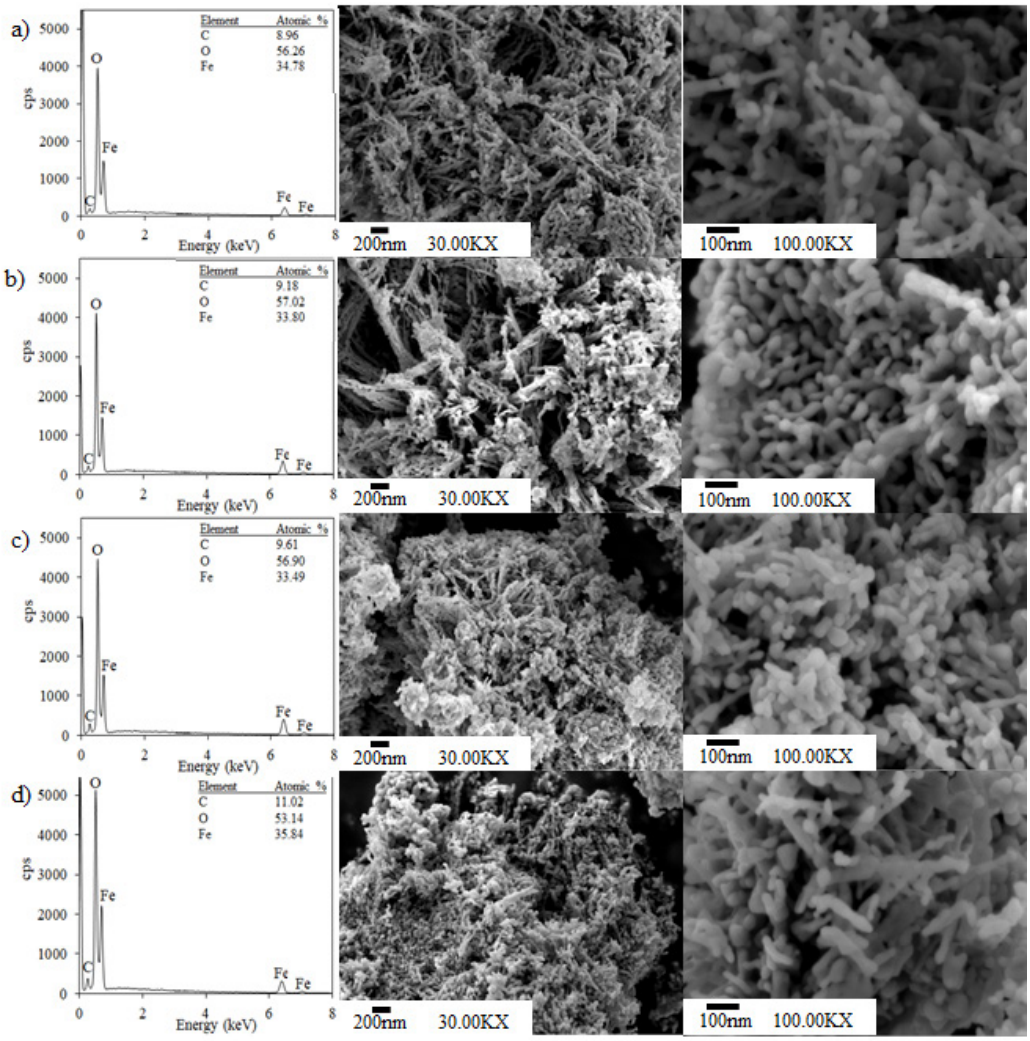

FIGURE 5. FESEM-EDX micrographs for a) α-Fe_2O_3, b) 4 hours of CO_2 adsorption on α-Fe_2O_3, c) 12 hours of CO_2 adsorption on α-Fe_2O_3, and d) 24 hours of CO_2 adsorption on α-Fe_2O_3

sonication assisted method was employed, a different precursor, precipitation agent and pH controller compared to Chen, Chen and Liu (2016) result in a different shape of iron(III) oxide. A coral-like morphology of α-Fe_2O_3 was reported to possess a significantly larger surface area compared to a nanorod shape (Kment et al. 2017) which could enhanced the adsorption capacity. The micrograph for the long CO_2 exposure on the nano coral-shaped α-Fe_2O_3 of 4, 12 and 24 hours were indistinct. The O element showed a general increase in the atomic % over the time except for 24 hours ascribed to the regional factor during the area was scanned. Nevertheless, the C element increases proportionally over the CO_2 adsorption time indicating the capability and potential of α-Fe_2O_3 to adsorb CO_2 for a long period.

Conclusions

The hydrolysis method was used to synthesize α-Fe_2O_3 with the precursor concentration of 2 M of $Fe(NO_3)_3 \cdot 9H_2O$ and calcination temperature of 450 °C. The CO_2 adsorption isotherm at 25 ℃ showed α-Fe_2O_3 obtain an adsorption capacity of 8.66 cm^3/g (17.00 mg/g) which is higher than bulk α-Fe_2O_3. The experimental data was analyzed using adsorption isotherm models such as Langmuir, Freundlich, Temkin and D-R. Experimental CO_2 adsorption isotherm at 25 ℃ fit well for all isotherm models but it was found the best fit with Freundlich isotherm model with an R^2 value of 0.9129. This implies the CO_2 adsorption process is favorable by having multilayer adsorption on the heterogeneous surface. The surface analyses were conducted for fresh α-Fe_2O_3 and after being exposed to CO_2. The XRD pattern showed lower intensities of the peaks might be due to the formation of the complexes carbonate. The IR spectra showed a greater intensity from 4 to 24 hours of CO_2 exposure, especially for the C-O and asymmetry O-C-O stretches for carbonate compound. The hydrolysis method was confirmed to generate a nano coral reef shaped of α-Fe_2O_3 that was observed through FESEM-EDX. The carbonate formation onto nano coral-shaped α-Fe_2O_3 was not distinct but the increment of the C element indicates the capability and potential of α-Fe_2O_3 in a long CO_2 adsorption time.

Acknowledgements

The authors wish to express gratitude for the research work supported by Universiti Putra Malaysia (GP-IPB/2019/9671302, GP/2020/9692700), 6300940 grant award under OCIM Sdn. Bhd. to Universiti Putra Malaysia and 230.PKIMIA.6711923 grant award under Ministry of Higher Education to Universiti Sains Malaysia.

References

Abu Tahari, M.N., Lahuri, A.H., Ghazali, Z., Samidin, S., Sulhadi, S.S., Dzakaria, N. & Yarmo, M.A. 2020. Application of octadecylamine-based adsorbent on carbon dioxide capture. *Materials Science Forum* 1010: 367-372.

Abu Tahari, M.N., Hakim, A., Marliza, T.S., Mohd, N.H. & Yarmo, M.A. 2017. XRD and CO_2 adsorption studies of modified silica gel with octadecylamine. *Materials Science Forum* 888: 529-533.

Ammendola, P., Raganati, F. & Chirone, R. 2017. CO_2 adsorption on a fine activated carbon in a sound assisted fluidized bed: Thermodynamics and kinetics. *Chemical Engineering Journal* 322: 302-313.

Andrade, R.G.D., Veloso, S.R.S. & Castanheira, E.M.S. 2020. Shape anisotropic iron oxide-based magnetic nanoparticles: Synthesis and biomedical applications. *International Journal of Biomolecular Sciences* 21: 1-25.

Baltrusaitis, J., Schuttlefield, J., Zeitler, E. & Grassian, V.H. 2011. Carbon dioxide adsorption on oxide nanoparticle surfaces. *Chemical Engineering Journal* 170: 471-481.

Chen, X.R., Chen, Z.M. & Liu, X.J. 2016. Study on the preparation of nanometer α-Fe_2O_3 by sonochemical hydrolysis method. *MATEC Web of Conference* 67: 06074.

Djomgoue, P., Siewe, M., Djoufac, E., Kenfack, P. & Njopwouo, D. 2012. Surface modification of Cameroonian magnetite rich clay with Eriochrome Black T. Application for adsorption of nickel in aqueous solution. *Applied Surface Science* 258: 7470-7479.

Hakim, A., Marliza, T.S., Abu Tahari, M.N., Wan Isahak, W.N.R., Yusop, M.R., Hisham, M.W.M. & Yarmo, M.A. 2016a. Studies on CO_2 adsorption and desorption properties from various types of iron oxides (FeO, Fe_2O_3, and Fe_3O_4). *Industrial & Engineering Chemistry Research* 55: 7888-7897.

Hakim, A., Marliza, T.S., Abu Tahari, M.N., Yusop, M.R., Hisham, M.W.M. & Yarmo, M.A. 2016b. Development of α-Fe_2O_3 as adsorbent and its effect on CO_2 capture. *Materials Science Forum* 840: 421-426.

Hakim, A., Yarmo, M.A., Marliza, T.S., Abu Tahari, M.N., Samad, W.Z., Yusop, M.R., Hisham, M.W.M. & Dzakaria, N. 2016c. The influence of calcination temperature on iron oxide (α-Fe_2O_3) towards CO_2 adsorption prepared by simple mixing method. *Malaysian Journal of Analytical Sciences* 20(6): 1286-1298.

Hakim, A., Abu Tahari, M.N., Marliza, T.S., Wan Isahak, W.N.R., Yusop, M.R., Hisham, M.W.M. & Yarmo, M.A. 2015a. Study of CO_2 adsorption and desorption on activated carbon supported iron oxide by temperature programmed desorption. *Jurnal Teknologi (Sciences & Engineering)* 77(33): 75-84.

Hakim, A., Wan Isahak, W.N.R., Abu Tahari, M.N., Yusop, M.R., Hisham, M.W.M. & Yarmo, M.A. 2015b. Temperature programmed desorption of carbon dioxide for activated carbon supported nickel oxide: The adsorption and desorption studies. *Advanced Materials Research* 1087: 45-49.

Isokoski, K., Poteet, C.A. & Linnartz, H. 2013. Highly resolved infrared spectra of pure CO_2 ice (15-75 K). *Astronomy and Astrophysics* 555: A85.

Kazansky, V., Borovkov, V., Serykh, A.I. & Bulow, M. 1999. First observation of the broad-range DRIFT spectra of carbon dioxide adsorbed on NaX zeolite. *Physical Chemistry Chemical Physics* 1: 3701-3702.

Khdary, N.H., Ghanem, M.A., Abdesalam, M.E. & Al-Garadah, M.M. 2018. Sequestration of CO_2 using Cu nanoparticles supported on spherical and rod-shape mesoporous silica. *Journal of Saudi Chemical Society* 22(3): 343-351.

Kment, S., Riboni, F., Pausova, S., Wang, L., Wang, L.Y., Han, H.K., Hubicka, Z., Krysa, J., Schmuki, P. & Zboril, R. 2017. Photoanodes based on TiO_2 and α-Fe_2O_3 for solar water splitting-superior role of 1D nanoarchitectures and of combined heterostructures. *Chemical Society Reviews* 46: 3716-3769.

Lahuri, A.H. & Yarmo, M.A. 2022. Study of CO_2 adsorption time for carbonate species and linear CO_2 formations onto bimetallic CaO/Fe_2O_3 by infrared spectroscopy. *Sains Malaysiana* 51(2): 507-517.

Lahuri, A.H., Mohd Yusuf, A., Adnan, R., Abdul Rahim, A., Waheed Tajudeen, N.F. & Nordin, N. 2022a. Kinetics and thermodynamic modeling for CO_2 capture using NiO supported activated carbon by temperature swing adsorption. *Biointerface Research in Applied Chemistry* 12(3): 4200-4219.

Lahuri, A.H., Yarmo, M.A., Abu Tahari, M.N. & Dzakaria, N. 2022b. Adsorption isotherm analysis for CO_2 capture using barium oxide impregnated iron(III) oxide by ultrasonic-assisted synthesis. *Key Engineering Materials* 908: 379-384.

Lahuri, A.H., Yarmo, M.A. & Abu Tahari, M.N. 2022c. Ultrasonic assisted synthesis of bimetal composite strontium oxide/iron(III) oxide for the adsorption isotherm analysis of CO_2 capture. *Lecture Notes in Mechanical Engineering* 175-195.

Lahuri, A.H., Adnan, R., Mansor, M.H., Waheed Tajudeen, N.F. & Nordin, N. 2020a. Adsorption kinetics for carbon dioxide capture using bismuth(III) oxide impregnated on activated carbon. *Malaysian Journal of Chemistry* 22(1): 33-46.

Lahuri, A.H., Michale Ling, N.K., Abdul Rahim, A. & Nordin, N. 2020b. Adsorption kinetics for CO_2 capture using cerium oxide impregnated on activated carbon. *Acta Chimica Slovenica* 67: 570-580.

Lahuri, A.H., Yarmo, M.A., Abu Tahari, M.N., Marliza, T.S., Tengku Saharuddin, T.S., Mark Lee, W.F. & Dzakaria, N. 2020c. Comparative adsorption isotherm for beryllium oxide/iron (III) oxide toward CO_2 adsorption and desorption studies. *Materials Science Forum* 1010: 361-366.

Lahuri, A.H., Yarmo, M.A., Marliza, T.S., Abu Tahari, M.N., Samad, W.Z., Dzakaria, N. & Yusop, M.R. 2017. Carbon dioxide adsorption and desorption study using bimetallic calcium oxide impregnated on iron(III) oxide. *Materials Science Forum* 888: 479-484.

Lassoued, A., Dkhil, B., Gadri, A. & Ammar, S. 2017. Control of the shape and size of iron oxide (α-Fe_2O_3) nanoparticles synthesized through the chemical precipitation method. *Results in Physics* 7: 3007-3015.

Lisjak, D. & Merteli, A. 2018. Anisotropic magnetic nanoparticles: A review of their properties, syntheses and potential applications. *Progress in Materials Science* 95: 286-328.

Mendoza, E.Y.M., Santos, A.S., Lopez, E.V., Drozd, V., Durygin, A., Chen, J.H. & Saxena, S.K. 2019. Iron oxides as efficient sorbents for CO_2 capture. *Journal of Materials Research and Technology* 8(3): 2944-2956.

Mohanraj, K. & Sivakumar, G. 2017. Synthesis of γ-Fe_2O_3 , Fe_3O_4 and copper doped Fe_3O_4 nanoparticles by sonochemical method. *Sains Malaysiana* 46(10): 1935-1942.

Mutch, G.A., Anderson, J.A., Walker, R., Cerrato, G., Morandi, S., Operti, L. &Vega-Maza, D. 2016. *In-situ* infrared spectroscopy as a non-invasive technique to study carbon sequestration at high pressure and high temperature. *International Journal of Greenhouse Gas Control* 51: 126-135.

Nambo, A. 2019. Nanowire based adsorbents/catalysts for CO_2 capture and utilization. Theses and Dissertations. University of Louisville.ThinkIR: the University of Louisville's Institutional Repository (Unpublished).

Qin, W.Q., Yang, C.R., Yi, R. & Gao, G.H. 2011. Hydrothermal synthesis and characterization of single-crystalline α-Fe2O3 nanocubes. *Journal of Nanomaterials* 2011: 159259.

Rashidi, N.A. & Yusup, S. 2017. Potential of palm kernel shell as activated carbon precursors through single stage activation technique for carbon dioxide adsorption. *Journal of Cleaner Production* 168: 474-486.

Sattler, K.D. 2011. *Handbook of Nanophysics: Nanoparticles and Quantum Dot*s. Boca Raton: CRC Press.

Shaba, E.Y., Jacob, J.O., Tijani, J.O. & Suleiman, M.A.T. 2021. A critical review of synthesis parameters affecting the properties of zinc oxide nanoparticle and its application in wastewater treatment. *Applied Water Science* 11(48): 1-41.

Tadic, M., Panjan, M., Tadic, B.V., Lazovic, J., Damnjanovic, V., Kopani, M. & Kopanja, L. 2019. Magnetic properties of hematite (α−Fe_2O_3) nanoparticles synthesized by sol-gel synthesis method: The influence of particle size and particle size distribution. *Journal of Electrical Engineering* 70: 71-76.

Wu, Z., Yang, S. & Wu, W. 2016. Shape control of inorganic nanoparticles from solution. *Nanoscale* 8: 1237-1259.

Zhong, W.H., Li, B., Maguire, R.G., Dang, V.T., Shatkin, J.A., Gross, G.M. & Richey, M.C. 2012. *Nanoscience and Nanomaterials: Synthesis, Manufacturing and Industry Impacts.* Pennsylvania: DEStech Publication.

*Corresponding author; email: azizulhakim@upm.edu.my